COO-3496-38
CONF-730823--22

Energy Dependence of Γ_f/Γ_n for the Nucleus ^{216}Rn*

H. Freiesleben†, H.C. Britt††, and J.R. Huizenga

Nuclear Structure Research Laboratory, University of Rochester, Rochester, New York, USA

ABSTRACT

The ^{209}Bi + ^{7}Li reaction has been used to determine experimentally Γ_f/Γ_n for the initial compound nucleus ^{216}Rn. Cross sections for the (^{7}Li,f) reaction were measured at bombarding energies between 24 and 34 MeV by detecting coincident fission fragments. All the other components of the total reaction cross section are due to (^{7}Li,xn), (^{7}Li,txn) and (^{7}Li,αxn) reactions. They were determined by observing known energy alpha particles from the short lifetime decays of various Rn, At and Po isotopes. The background due to prompt reaction particles was eliminated by using a pulsed ^{7}Li-beam and detecting the decay particles between beam pulses. Correction for the effects of second chance fission were obtained from measurements of cross sections for the (^{6}Li,f) and (^{6}Li,xn) reactions at appropriate energies. The results give a direct measurement of Γ_f/Γ_n since both fission and neutron evaporation cross sections were determined. The experimental values of Γ_f/Γ_n for ^{216}Rn and earlier data for ^{210}Po are analyzed with a J dependent statistical model and the effect of incorporating an enhancement of the level density at the saddle point due to coupling to collective rotations is investigated. Fission barriers extracted with a variety of assumptions about the level densities are compared with theoretical predictions.

* Work supported in part by the U.S. Atomic Energy Commission and the National Science Foundation

† On leave of absence from Fachbereich Physik, Universität Marburg, W. Germany

†† Permanent address: Los Alamos Scientific Laboratory, Los Alamos, New Mexico

DISCLAIMER

Energy Dependence of Γ_f/Γ_n for the Nucleus ^{216}Rn*

H. Freiesleben†, H.C. Britt††, and J.R. Huizenga

Nuclear Structure Research Laboratory, University of Rochester, Rochester, New York, USA

1. INTRODUCTION

Previous measurements[1-4] of fission excitation functions for nuclei in the rare earth and lead region have been used to determine fission barrier heights for a range of nuclei from $^{173}_{71}Lu$ through $^{213}_{85}At$. These results, which were obtained from reactions with alpha particle and proton beams, have shown[5] that the fission barrier decreases rapidly from 23.3 MeV for $^{209}_{83}Bi$ to 17.0 MeV for $^{213}_{85}At$. This change in threshold is due primarily to the decreasing influence of the strong spherical shell at Z=82, N=126 on the ground state mass. Due to a lack of target isotopes with reasonable lifetimes, there are no fission barrier measurements between $^{213}_{85}At$, which has a spherical equilibrium shape with a barrier of 17.0 MeV and $^{227}_{88}Ra$, which has a deformed equilibrium shape with a barrier of 8.1 MeV[6].

With the availability of high energy heavy ion beams, it is possible to study the fission barrier of nuclei with Z>85 making use of stable Pb and Bi targets. One particularly

* Work supported in part by the U.S. Atomic Energy Commission and the National Science Foundation

† On leave of absence from Fachbereich Physik, Universität Marburg, W. Germany

†† Permanent address: Los Alamos Scientific Laboratory, Los Alamos, New Mexico

advantageous reaction is $^{209}Bi + {}^{7}Li \rightarrow {}^{216}_{86}Rn$. In this case, the residual nuclei formed by multiple neutron evaporation are easily observed short-lived alpha particle emitters. By measuring both the fission cross section and the cross sections for forming the residual products $^{216-x}Rn$ from xn reactions, it is possible to obtain a direct measure of Γ_f/Γ_n. This method can be contrasted with earlier measurements[1-4] where Γ_f/Γ_n was determined from a measured fission cross section and a calculated total reaction cross section.

From the experimental Γ_f/Γ_n measurements, the extraction of the height of the fission barrier requires a statistical model to calculate Γ_f and Γ_n. Recent calculations[5,7] have shown that it is essential to include shell effects in the Γ_n calculation in order to account for the influence of the double shell closure. In this connection, Moretto et al.[5] have shown that it is possible to reproduce the shapes of the experimental excitation functions without specifically considering the effects of shells at the saddle point. Vandenbosch and Mosel[7] attempted an absolute calculation of Γ_f/Γ_n incorporating shell effects in both Γ_f and Γ_n and using theoretically calculated heights for the fission barriers. However, both these calculations neglected a fundamental difference between the level densities for the deformed saddle point used in Γ_f and the spherical ground state appropriate for Γ_n. In particular for a deformed nucleus the level densities can be enhanced by coupling to collective degrees of freedom.

In this paper, we report direct experimental measurements of Γ_f/Γ_n for ^{216}Rn. The results are analyzed with a statistical model that includes an improved microscopic calculation of Γ_f which explicitly contains the effects of collective rotations on the level density at the saddle point. In addition, Γ_f/Γ_n is calculated as a function of J and then weighted over the distribution of angular momenta in the entrance channel. Calculations from this statistical model are compared to the experimental ^{216}Rn data and also to the more extensive data[3] reported previously for the compound nucleus ^{210}Po produced by the $^{206}Pb + \alpha$ reaction. The data are first compared to an absolute prediction which includes both theoretical level densities incorporating realistic shell corrections and the corresponding theoretical value for the fission barrier height[8]. In an alternate approach the height of the fission barrier and a normalization factor are deduced empirically from a fit to the experimental data.

2. EXPERIMENTAL PROCEDURE

Bismuth targets were bombarded with $^{6,7}Li$-projectiles from the Emperor tandem Van de Graaff with energies of 25 to 34 MeV. The fission cross section was measured using a d.c. Li-beam. Fission fragments were detected in coincidence

in high geometry surface barrier detectors. It was necessary to detect fission fragment pairs in order to measure this small cross section in presence of the intense elastic scattering.

If the compound nucleus does not fission, multiple neutron emission leads to the residual Rn-nuclei, which are shown in fig. 1. Since all of these nuclei are α-emitters, their formation cross sections are easily determined by measuring their α-activities. The identification of the α-groups is unique, based on the known α-energies and half-lives, which range from about hundred nanoseconds to minutes. Using a pulsed Li-beam to produce the Rn-isotopes, we could measure the α-activities between beam pulses with standard surface barrier detectors essentially free of background due to prompt α-groups. All expected α-groups were found, including those following the (^{7}Li,xn) reactions and a variety of transfer reactions leading to Po, At and Bi isotopes as shown in fig. 1. All reaction-channels together give a complete measurement of the total reaction cross section, which will be discussed elsewhere[9].

3. RESULTS

The excitation function for the compound nucleus formation is shown in fig. 2, together with the fission and multiple neutron evaporation decay channels. To obtain values for Γ_f/Γ_n as close to the fission barrier as possible, the measurements were done mainly below the Coulomb barrier of about 33 MeV. Hence the compound nucleus formation cross section and the resulting cross sections of the various exit channels are mainly controlled by the Coulomb barrier, and it is very difficult to extend the measurements to lower incident energies.

The total fission cross sections are calculated from the differential cross section at 90°. A measurement of the anisotropy at 33 MeV gave $W(165°)/W(90°) = 1.19\pm0.15$. Hence, isotropy was assumed over the whole energy range. The fission excitation function obtained for ^{6}Li yields a larger cross section at a fixed incident energy than ^{7}Li. This is mainly due to the Q-value of the ^{209}Bi + ^{6}Li reaction, which is 660 keV larger than that for the ^{209}Bi + ^{7}Li reaction, and partially due to the change of the fissility parameter in going from ^{216}Rn to ^{215}Rn.

The ^{6}Li induced fission cross sections were used to correct the ^{7}Li induced fission data for the contribution of second chance fission. An effect of less than 6% was obtained at our highest incident ^{7}Li energy of 34 MeV.

The results for the (^{7}Li,xn) cross sections show the dominance of evaporation of three neutrons in the measured range of incident energies, with the 4n threshold at approximately 30 MeV ^{7}Li energy. The cross section for one neutron emission is below our detection system efficiency of $\sim$1μb and hence not measured.

The experimental ratio Γ_f/Γ_n as a function of the compound nucleus excitation energy is displayed in fig. 3. This ratio varies only slowly with excitation energy since one is still well above the fission barrier, but nevertheless deep in the Coulomb barrier. The theoretical curves included in the figure will be discussed later.

4. THEORY

The calculation of the fission width has been performed using the formula of Bohr and Wheeler[10] which has been generalized to include a J dependence,

$$\Gamma_f(J) = \frac{D(J)}{2\pi}\int_0^{E-E_f} \rho_f(E-E_f-\varepsilon,J)\,d\varepsilon \qquad (1)$$

where E_f is the effective fission barrier, ρ_f the level density at the saddle point deformation for a total angular momentum J and D(J) the level spacing in the compound nucleus at excitation energy E and angular momentum J.

On the neutron side, the J-dependent neutron width $\Gamma_n(J)$ is given by

$$\Gamma_n(J) = \frac{D(J)}{2\pi}\int_0^{E-B_n} \sum_{L=0}^{L_{max}} T_L \sum_{S=|J-L|}^{J+L} \sum_{I=|S-1/2|}^{S+1/2} \rho_n(E-B_n-\varepsilon,I)\,d\varepsilon \qquad (2)$$

where B_n is the neutron binding energy in the compound nucleus and ρ_n the level density for total angular momentum I in the residual nucleus. The neutron transmission coefficients[11] T_L are those describing the formation of the compound nucleus at excitation energy E via neutron capture by the residual nucleus. These calculations are straightforward, if the J-dependent level densities are provided, a problem which shall be discussed in greater detail.

Given a set of single particle spectra, a realistic state density calculation with the inclusion of nuclear pairing can be performed using the partition function method[12]. Details on the calculations may be found in ref. 13. Single particle levels of Möller and Nix[8] were used to obtain state densities $\omega(E)$ for the spherical nuclei ^{209}Po and ^{215}Rn. The level densities $\rho(E,J)$, which later are used to calculate $\Gamma_n(J)$ following eq. (2), are obtained from the relation

$$\rho(E,J) = \frac{J+1/2}{\sqrt{2\pi}\,\sigma^3(E)}\,\omega(E)\cdot\exp\left(-\frac{J(J+1)}{2\sigma^2(E)}\right) \qquad (3)$$

where the spin cut-off factor $\sigma^2(E)$ is also calculated microscopically.

For the fissioning nuclei ^{210}Po and ^{216}Rn, the state densities $\omega(E)$ were calculated using Möller and Nix's[8] single particle levels at the saddle point deformation. In the case of ^{210}Po, single particle levels for both a symmetric and an asymmetric saddle point deformation were used. For the deformed saddle point the level density is enhanced by coupling to low lying collective excitations as described by Bjørnholm, Bohr and Mottelson[14]. For an axially symmetric shape where only the coupling to collective rotations is considered the level density can be written as:

$$\rho_c(E,J) = \frac{\omega_K(E)\hbar}{\sqrt{8\pi \vartheta_{\parallel} T}} \sum_{K=-J}^{+J} \exp\{-\frac{\hbar^2K^2}{2\vartheta_{\parallel} T} - \frac{\hbar^2}{2\vartheta_{\perp} T}[J(J+1)-K^2]\} \qquad (4)$$

where $\omega_K(E)$ is the state density calculated microscopically in the K formalism appropriate for a deformed nucleus and the analogous cutoff factor $\sigma_K^2(E) = \vartheta_{\parallel} T/\hbar^2$ is also calculated microscopically. In the actual calculations a rigid-body estimate for the perpendicular moment of inertia, $h^2/2\vartheta_{\perp} = 2.5$ keV, was used. If it is assumed that $\omega_K(E)$ contains all the available states (i.e. no enhancement due to rotations) then Sano and Kawai[15] have shown that the level density becomes:

$$\rho_D = \frac{\hbar^2}{\vartheta_{\perp} T} \cdot \rho_c \qquad (5)$$

Previous calculations[5,7] have essentially used eq.(5) with the further approximation that $\sigma^2 \sim \sigma_K^2 \sim \hbar^2/\vartheta_{\perp} T$, where σ^2 is the spin cutoff factor for the spherical nucleus formed in neutron emission. In this limit the spin cutoff factors cancel and the final Γ_f/Γ_n expressions are J independent.

Since the experimentally determined Γ_f/Γ_n is a weighted sum over the distribution of angular momenta in the entrance channel, a final summation is needed.

$$\left\langle \frac{\Gamma_f}{\Gamma_n} \right\rangle = \frac{\sum_{J=0}^{J_{max}} P_J \cdot (\Gamma_f/\Gamma_n)_J}{\sum_{J=0}^{J_{max}} P_J}$$

where P_J is the probability for forming the compound nucleus with angular momentum J. These probability coefficients are calculated with transmission coefficients from a parabolic approximation of the potential barrier as introduced by Thomas[16]. The ratio of $(\Gamma_f/\Gamma_n)_J/(\Gamma_f/\Gamma_n)_{J=0}$ as a function

of J for three different excitation energies in the compound nucleus ^{210}Po are shown in Fig. 4. One interesting feature of these curves is that at the lower excitation energies the higher angular momentum values favor neutron emission. This is a result of the large difference in the fission barrier and neutron threshold and the corresponding difference in the appropriate spin cutoff factors.

5. DISCUSSION

The statistical model was first used for an absolute prediction of Γ_f/Γ_n for ^{210}Po and ^{216}Rn using the single particle levels and theoretical barriers from Möller and Nix[8]. These calculations, therefore, contain no adjustable parameters. The results are compared to experimental data in Figs. 3 and 5. The absolute calculations tend to reproduce experimental results near threshold but rise too steeply and give too large values for Γ_f/Γ_n at high excitation energies. This comparison may indicate that the present statistical model yields an incorrect energy dependence for Γ_f/Γ_n. Alternately, the theoretically calculated barriers and level densities may be incorrect.

Since comparisons for actinide nuclei have shown deviations of up to 2 or 3 MeV in some cases between experimental fission barriers and those calculated theoretically by Möller and Nix[8], it is also interesting to investigate an alternative approach where the height of the fission barrier, E_f, and a normalization factor, N_f, are extracted from a fit to the experimental data. The results of these fits are shown in Figs. 6 and 7 and the parameters obtained are listed in Table I. In these fits level densities from both eqs.(4) and (5) were used. For ^{210}Po, single particle levels for both symmetric and asymmetric saddle points were used.

In Figs. 6 and 7 it is shown that the shapes of the experimental Γ_f/Γ_n functions are well described in all cases. However, the parameters E_f and N_f depend both on the single particle spectrum and the type of level density formula which is used. For ^{210}Po the use of symmetric or asymmetric saddle point single particle levels results in only a small difference in the fitted parameters. In contrast the two different forms for the level density give N_f values which change by a factor of about 400 and fitted values of E_f which change by ~0.8 MeV. Using the level density including collective rotations, N_f values in the range 10^{-2} to 10^{-3} are obtained rather than the expected values of ~1. Conversely, the approach (eq. 5) which neglects these new levels gives a normalization factor of ~1. For the ^{216}Rn case the collective level density gives $N_f \sim 1/20$, whereas, the other approach gives $N_f \sim 20$ so that $N_f \sim 1$ is between the two extremes.

Operationally the theoretical energy dependent values of Γ_f/Γ_n are compared with the experimental ratios of this quantity at several energies. Since the theoretical values of Γ_f/Γ_n depend on three different variables, namely the fission barrier and the level densities of both the deformed saddle nucleus and the spherical nucleus following neutron emission, it is not possible to unambiguously determine both N_f and E_f. Hence, it is not possible to verify the necessity of introducing the deformed nucleus level density given by eq. 4 for estimating Γ_f/Γ_n at our excitation energies. If, however, the level density incorporating the enhancement due to collective rotations at the saddle point is correct then these results suggest that Γ_n is significantly underestimated at high excitation energies[17]. Whether this underestimate is a function of excitation energy depends on the value chosen for E_f. An underestimate of Γ_n could arise in two ways 1) through a neglect of possible couplings to collective vibrations at higher E^* (although this effect is also neglected in Γ_f) or 2) because of an overestimate of the shell effect on the level density in this region. This second possiblilty is consistent with the trend that the theoretical calculations[8] underestimate the ground state mass of ^{210}Po by 1.6 MeV and by 0.3 MeV for ^{216}Rn and the resulting N_f values are ~10 times smaller for ^{210}Po than for ^{216}Rn.

We would like to thank J.R. Nix and P. Möller for supplying the single particle spectra used in our calculations, and A.N. Behkami for assisting in the microscopic state density calculations.

Table 1. Fission barriers and normalization factors based on fits of the shape of Γ_f/Γ_n with two different forms of the level density for the deformed saddle nucleus. Theoretical barriers in the last column are based on experimental ground state masses.

	Values obtained with eq. 4		Values obtained with eq. 5		Theoretical[a] barrier
NUCLEUS	E_f(MeV)	N_f	E_f(MeV)	N_f	E_f(MeV)
^{210}Po (asym. saddle)	$19.5^{+.8}_{-.8}$	$1.9\cdot10^{-2}$ $6.0\cdot10^{-3}$ $2.0\cdot10^{-3}$	$20.2^{+.8}_{-.8}$	6.6 2.2 0.67	22.1
^{210}Po (sym. saddle)	$19.1^{+.8}_{-.8}$	$4.5\cdot10^{-3}$ $1.5\cdot10^{-3}$ $0.5\cdot10^{-3}$	$20.0^{+.8}_{-.8}$	2.5 0.75 0.23	22.1
^{216}Rn (asym. saddle)	$13.1^{+1.0}_{-1.0}$	$20\cdot10^{-2}$ $4.8\cdot10^{-2}$ $1.1\cdot10^{-2}$	$13.8^{+1.0}_{-1.0}$	64 16 4.6	14.8

(a) ref. 8. In figs. 3 and 5 the theoretical values of Γ_f/Γ_n were calculated with these theoretical fission barriers and no other adjustable parameters.

REFERENCES

[1] J.R. HUIZENGA, R. CHAUDHRY, and R. VANDENBOSCH, Phys. Rev. 126(1962)210.

[2] D.S. BURNETT, R.C. GATTI, F. PLASIL, P.B. PRICE, W.J. SWIATECKI, and S.G. THOMPSON, Phys. Rev. 134 (1964)B952.

[3] A. KHODAI-JOOPARI, University of California, Lawrence Radiation Laboratory Report UCRL-16489(1966).

[4] G.M. RAISBECK and J.W. COBBLE, Phys. Rev. 153(1967)1270.

[5] L.G. MORETTO, S.G. THOMPSON, J. ROUTTI, and R.C. GATTI, Phys. Letts. 38B(1972)471.

[6] H. GROENING and W. LOVELAND, Third International Conference on the Physics and Chemistry of Fission, paper IAEA/SM-174/81.

[7] R. VANDENBOSCH and U. MOSEL, Phys. Rev. Letts. 28(1972) 1726.

[8] P. MÖLLER and J.R. NIX, Third International Conference on the Physics and Chemistry of Fission paper IAEA/SM-174/202, and private communication.

[9] H. FREIESLEBEN, H.C. BRITT, and J.R. HUIZENGA, to be published.

[10] N. BOHR and J.A. WHEELER, Phys. Rev. 56(1939)426.

[11] E.H. AUERBACH and F.G.J. PEREY, Brookhaven National Laboratory Report BNL 765(T-286).

[12] J.R. HUIZENGA and L.G. MORETTO, Am. Rev. Nucl. Sci. Vol.22, 1972, p.427 and refs. given there.

[13] A.N. BEHKAMI and J.R. HUIZENGA, University of Rochester, Nuclear Structure Research Laboratory Report, UR-NSRL-72 (1973).

[14] S. BJØRNHOLM, A. BOHR and B.R. MOTTELSON, Third International Conference on the Physics and Chemistry of Fission, paper IAEA/SM-174/205.

[15] M. SANO and M. WAKAI, Prog. Theor. Phys. 48(1972)160.

[16] D.T. THOMAS, Phys. Rev. 116(1959)703.

[17] The evidence in support of the level density given by eq. 4 for reproducing the experimental level densities of deformed nuclei at the neutron binding energy is discussed in a separate paper by J.R. HUIZENGA, A.N. BEHKAMI, H.C. BRITT and H. FREIESLEBEN, preprint.

FIGURE CAPTIONS

Fig. 1. Portion of the nuclide chart in the region A=209 to 216. Listed are the ^{7}Li-induced reactions on ^{209}Bi populating the residual nuclei which were observed by their α-decay properties.

Fig. 2. Left side: Cross sections for the dominant decay channels of the compound nucleus ^{216}Rn as a function of projectile energy. Right side: Comparison of the decay of ^{215}Rn and ^{216}Rn by fission and multiple neutron evaporation as a function of the Li-ion energy incident on ^{209}Bi.

Fig. 3. The ratio Γ_f/Γ_n for ^{216}Rn as a function of excitation energy. The curve is calculated using eq. 4 and a fission barrier[8] of 14.8 MeV without additional free parameters.

Fig. 4. The dependence of Γ_f/Γ_n on angular momentum J for the compound nucleus ^{210}Po at three excitation energies. These results are based on eq. 4 and an asymmetric saddle with a fission barrier of 22.1 MeV.

Fig. 5. The ratio Γ_f/Γ_n for ^{210}Po as a function of excitation energy. The curves with level densities based on the single particle spectra for an asymmetric and a symmetric saddle point deformation are calculated using eq. 4 and a fission barrier of 22.1 MeV in both cases without additional free parameters.

Fig. 6. The ratio Γ_f/Γ_n for ^{216}Rn as a function of excitation energy. The curves for the different barriers are calculated with eq. 5. The normalization constants used to reproduce the experimental magnitude of Γ_f/Γ_n are given in table 1.

Fig. 7. The ratio Γ_f/Γ_n for ^{210}Po as a function of excitation energy. The curves are calculated with eq. 5, using level densities based on the single particle spectra for an asymmetric and a symmetric saddle point deformation. Fission barrier heights of 20.2 MeV and 20.0 MeV were used respectively. The normalization constants used to reproduce the experimental magnitude of Γ_f/Γ_n are given in table 1.

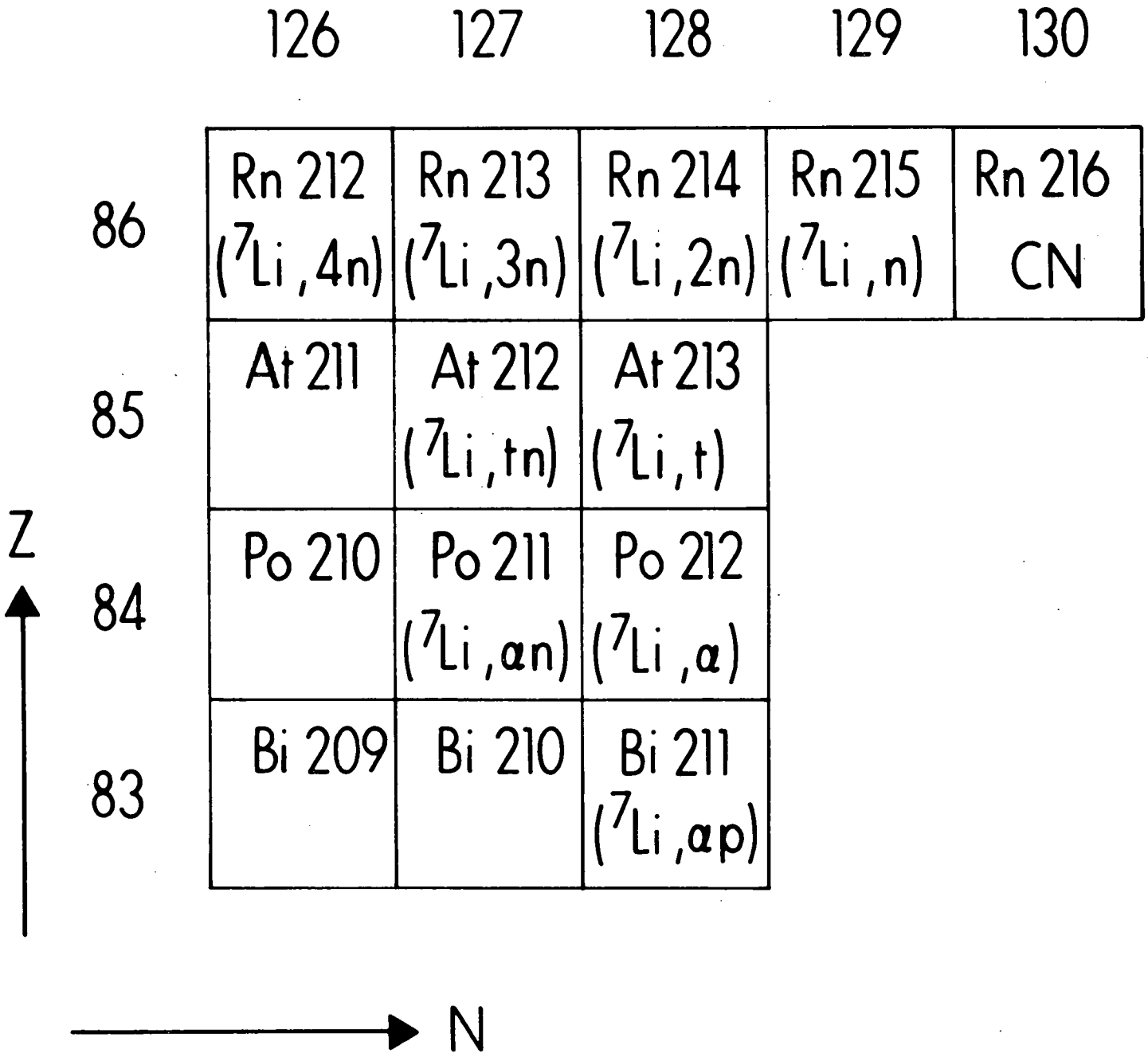
126
127
128
129
130
86
85
84
83
Rn 212 (^{7}Li, 4n)
Rn 213 (^{7}Li, 3n)
Rn 214 (^{7}Li, 2n)
Rn 215 (^{7}Li, n)
Rn 216 CN
At 211
At 212 (^{7}Li, tn)
At 213 (^{7}Li, t)
Po 210
Po 211 (^{7}Li, αn)
Po 212 (^{7}Li, α)
Bi 209
Bi 210
Bi 211 (^{7}Li, αp)
Z
N

Figure 1

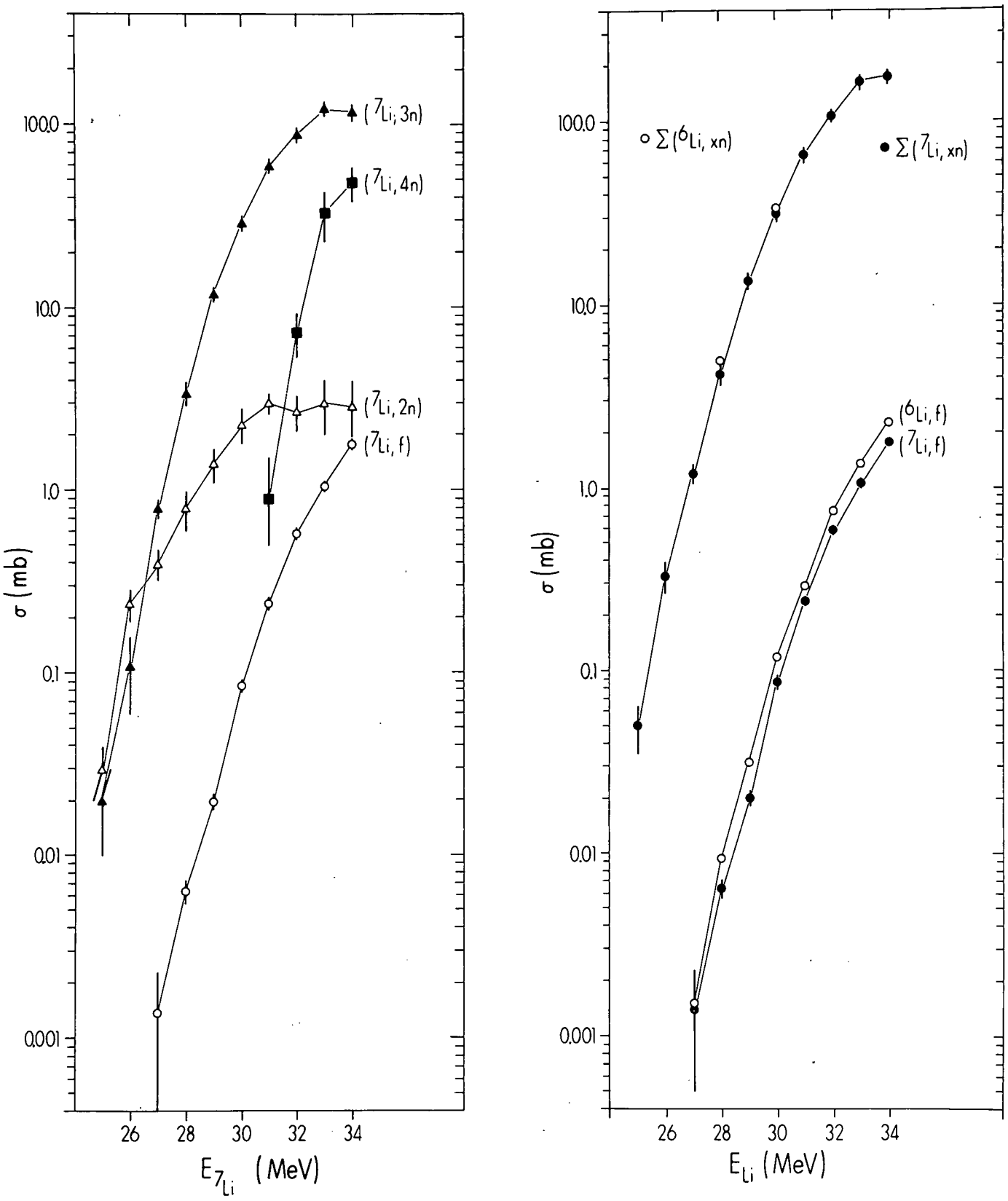
100.0
10.0
1.0
0.1
0.01
0.001
σ (mb)
(7Li, 3n)
(7Li, 4n)
(7Li, 2n)
(7Li, f)
26
28
30
32
34
E7Li (MeV)
Σ(6Li, xn)
Σ(7Li, xn)
(6Li, f)
(7Li, f)
ELi (MeV)

Figure 2

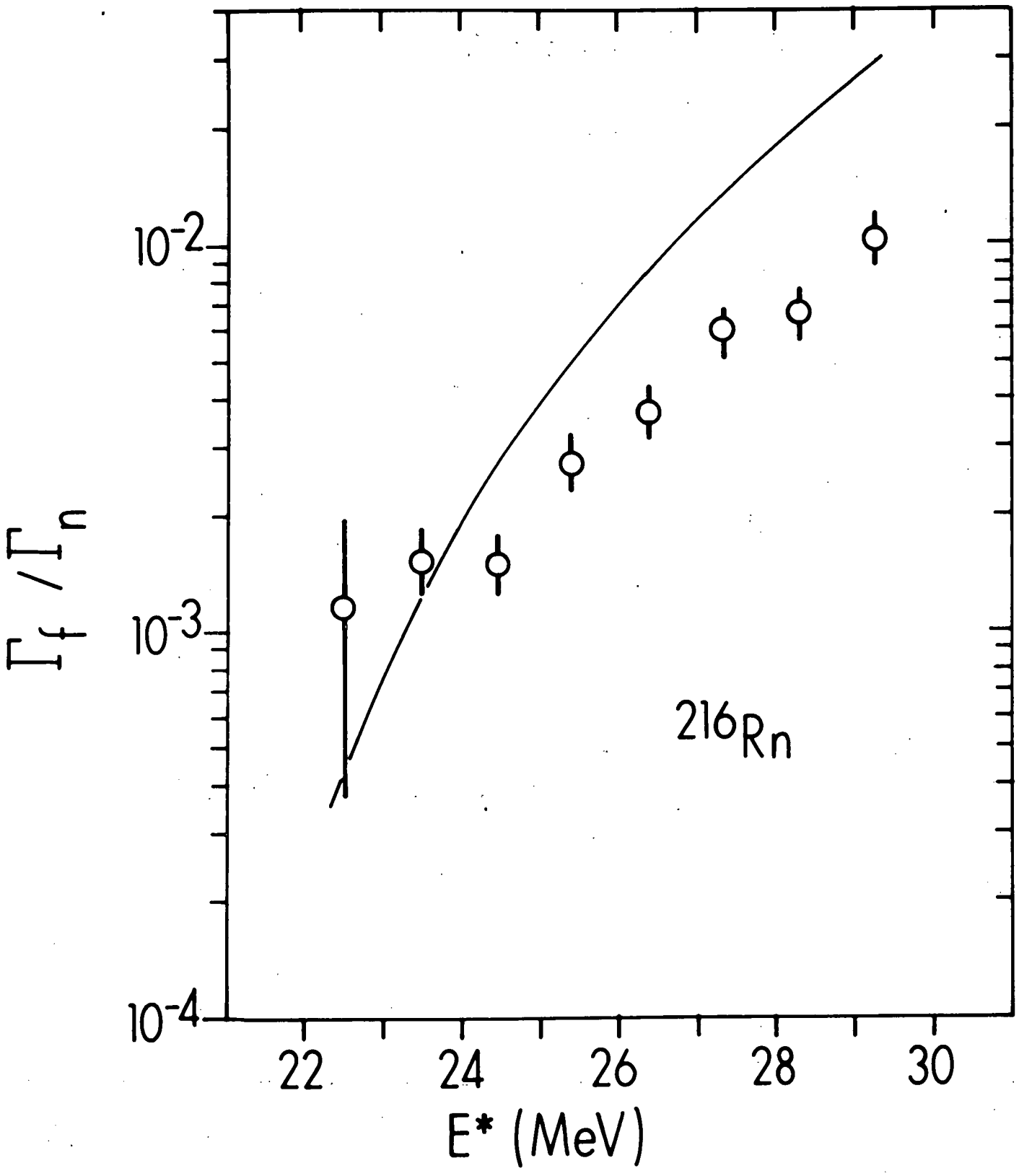

Figure 3

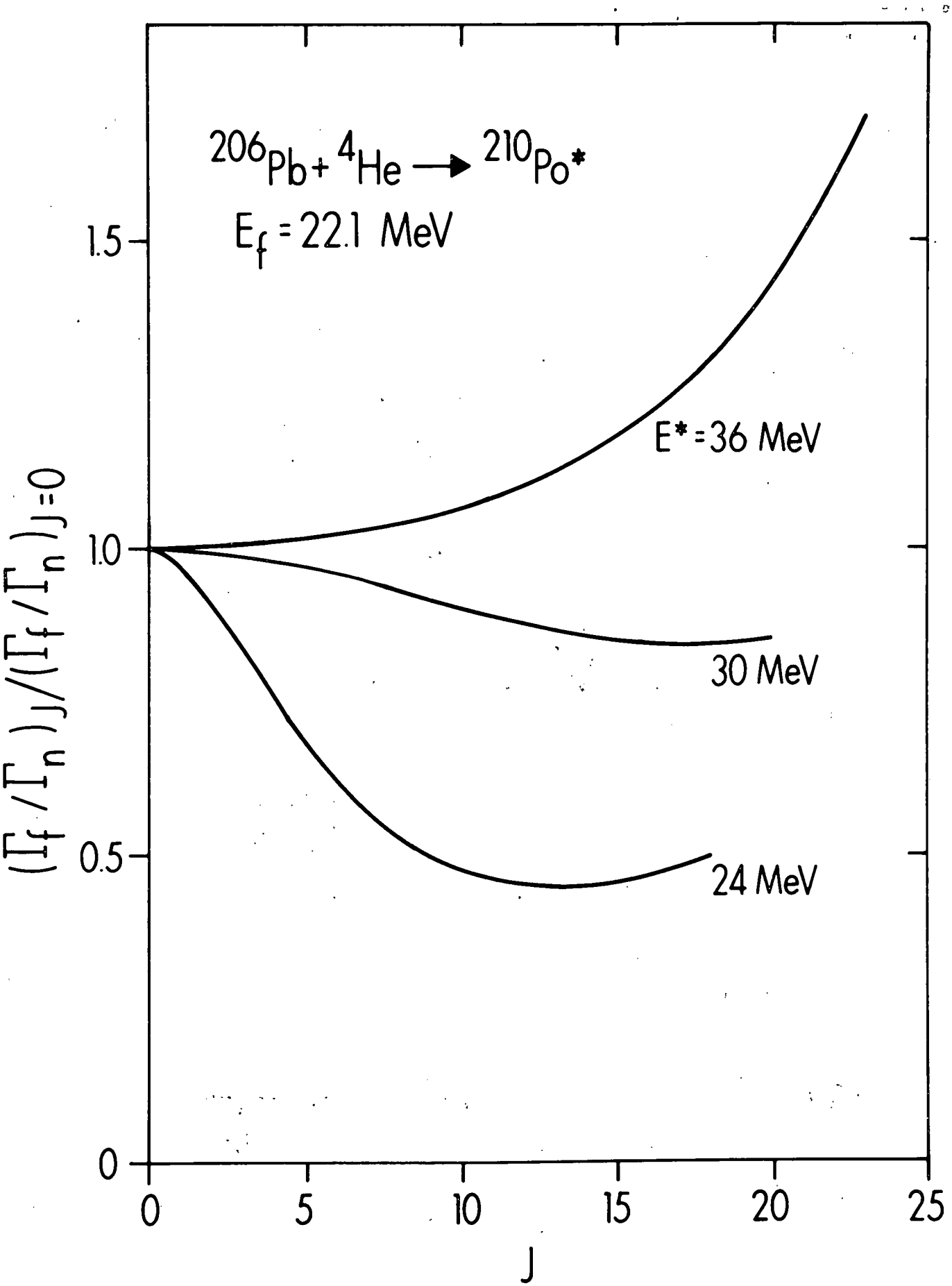
$^{206}Pb + ^{4}He \rightarrow ^{210}Po^{*}$
$E_f = 22.1$ MeV
$E^* = 36$ MeV
30 MeV
24 MeV
$(\Gamma_f/\Gamma_n)_J/(\Gamma_f/\Gamma_n)_{J=0}$
1.5
1.0
0.5
0
0
5
10
15
20
25
J

Figure 4

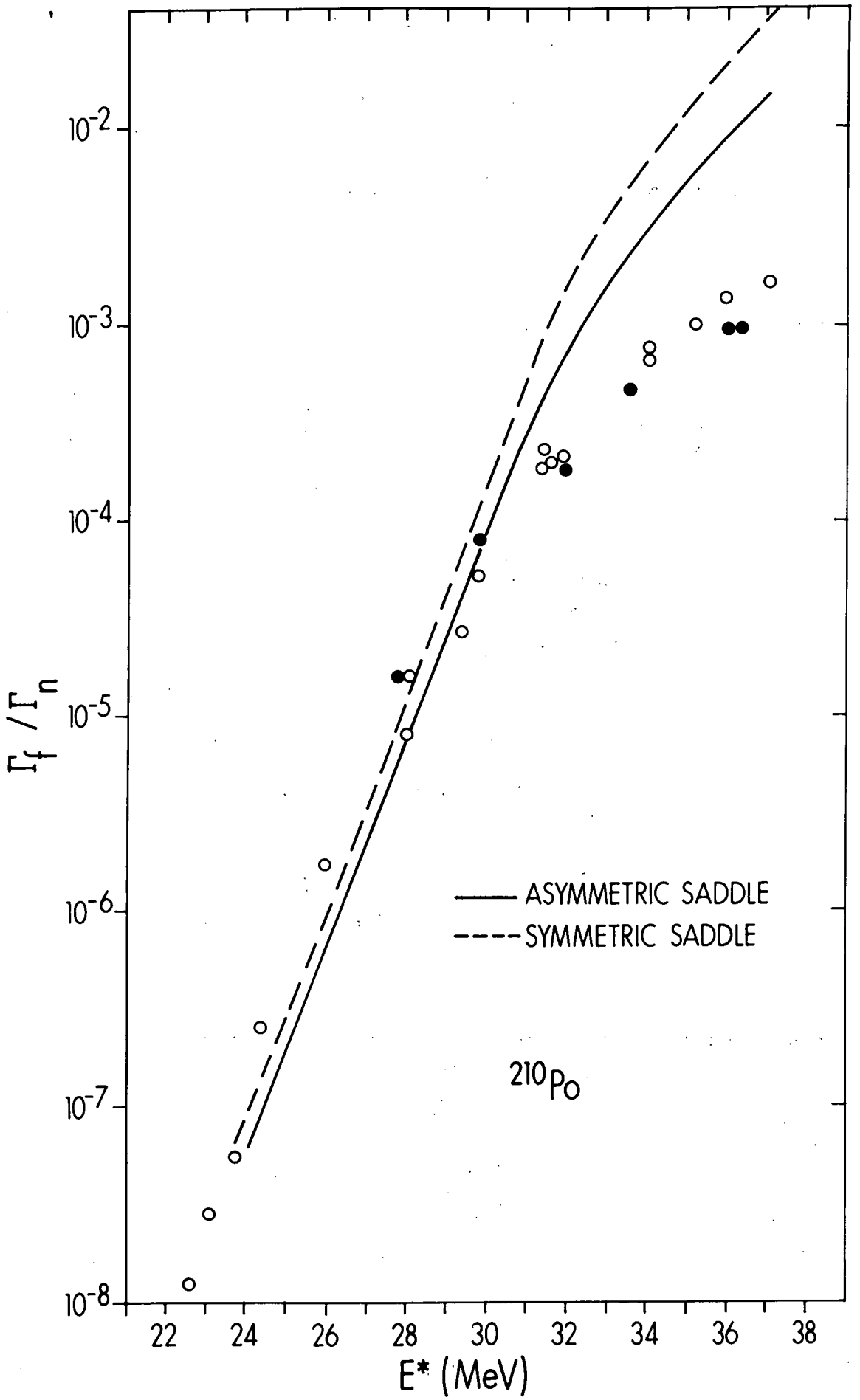
10^{-2}
10^{-3}
10^{-4}
10^{-5}
10^{-6}
10^{-7}
10^{-8}
Γ_f / Γ_n
22
24
26
28
30
32
34
36
38
E* (MeV)
ASYMMETRIC SADDLE
SYMMETRIC SADDLE
^{210}Po

Figure 5

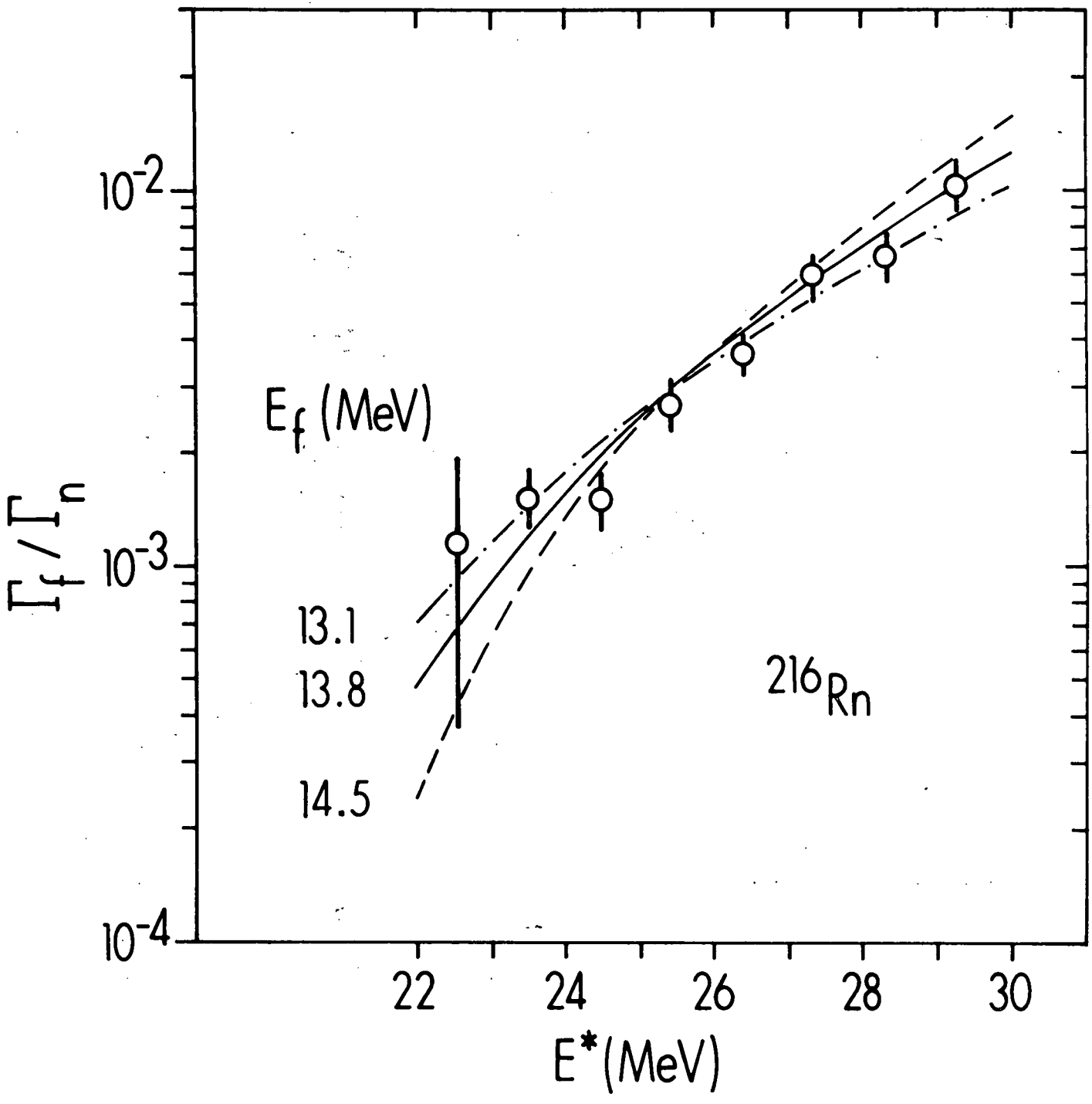
10^{-2}
10^{-3}
10^{-4}
Γ_f / Γ_n
E_f (MeV)
13.1
13.8
14.5
^{216}Rn
22
24
26
28
30
E*(MeV)

Figure 6

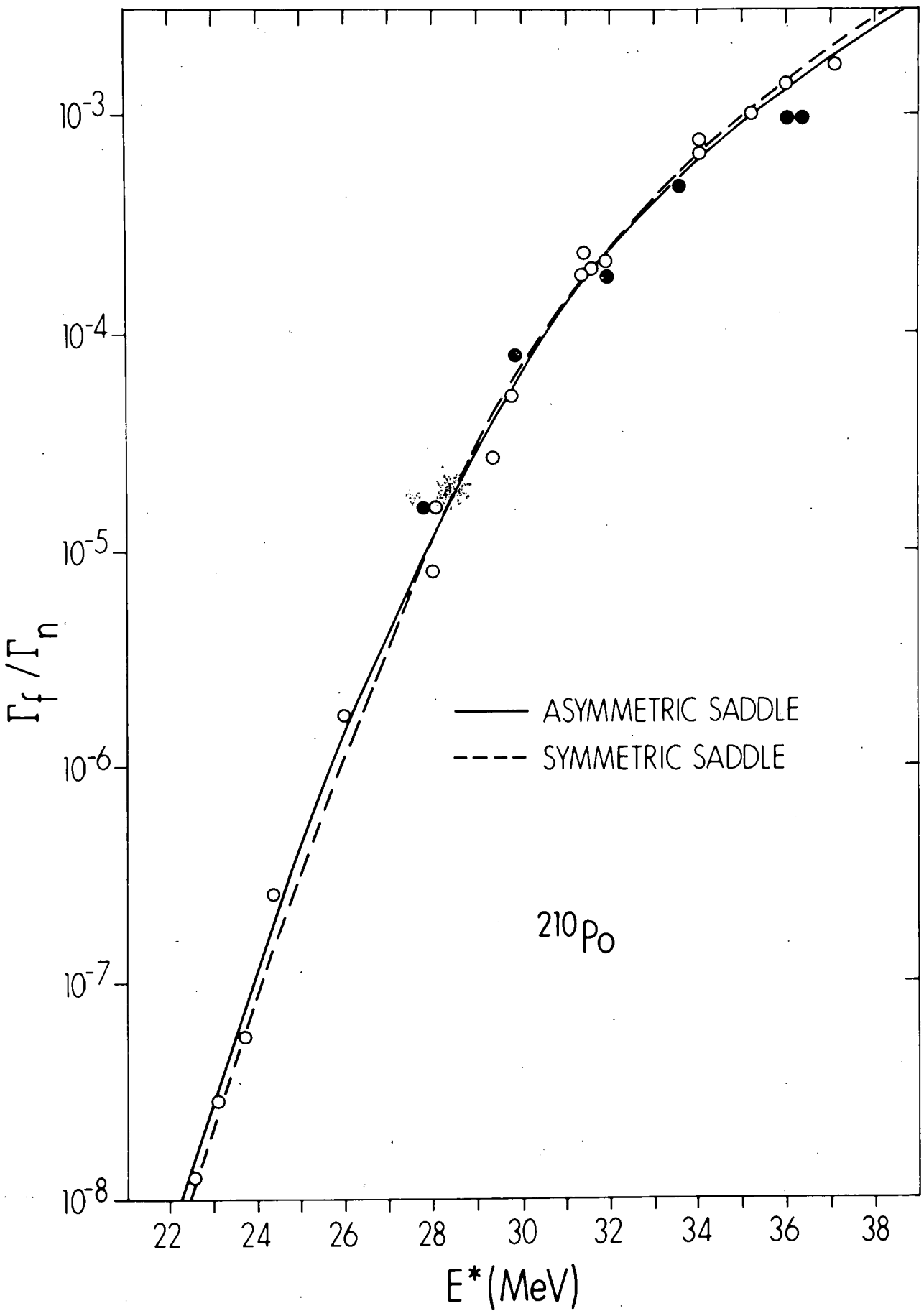
10^{-3}
10^{-4}
10^{-5}
10^{-6}
10^{-7}
10^{-8}
Γ_f / Γ_n
ASYMMETRIC SADDLE
SYMMETRIC SADDLE
^{210}Po
22
24
26
28
30
32
34
36
38
E*(MeV)

Figure 7